A new method for the identification of the parameters of the Dahl model

Isabel García-Baños and Fayçal Ikhouane

Universitat Politècnica de Catalunya, Departament de Matemàtiques, Escola Universitària d'Enginyeria Tècnica Industrial de Barcelona, Comte d'Urgell, 187, 08036, Barcelona, Spain.

E-mail: isabel.garcia.banos@upc.edu and faycal.ikhouane@upc.edu

Abstract. Friction is a nonlinear phenomenon that is present in many areas of science and engineering. It has static and dynamic characteristics. This paper deals with a dynamic model of friction, namely the Dahl model. More precisely, this paper proposes a new methodology for the identification of the parameters of the Dahl model. It is shown that, in the absence of noise, the identified parameters are equal to the real ones. Numerical simulations are carried out to illustrate the identification methodology.

1. Introduction and problem statement

Friction is a nonlinear phenomenon that originates from the contact of two bodies which makes it present in many areas of science and engineering, including mechanics [10], magnetics [1], and robotics [4] among others. Friction has two types of characteristics, static and dynamic. The static characteristics of friction include the stiction friction, the kinetic force (the Coulomb force), the viscous force, and the Stribeck effect which are functions of steady state velocity. Dynamic friction models capture properties that cannot be captured by typical static friction models; for instance, presliding displacement related to the elastic and plastic deformations of asperities (roughness features), frictional lag, that is the delay in the change of friction force as a function of a change of velocity, and stick-slip motion, which is the spontaneous jerking motion that can occur while two objects are sliding over each other [3].

This paper deals with a dynamic model of friction, namely the Dahl model [6]. More precisely, the aim of the paper is to propose a methodology for the identification of the parameters of the Dahl model. To explain this model and state the problem under study, we have organized this introduction into three subsections. In Section 1.1 we introduce the Coulomb model which is a necessary step to understand the Dahl model. Section 1.2 introduces the Dahl model in relation with the Coulomb model. Finally, the problem statement is provided in Section 1.3.

1.1. The Coulomb model

Consider the cube of Figure 1 resting on an inclined plane with slope θ.
Using Newton's second law we get

$$m\ddot{x} = P_x - F \tag{1}$$

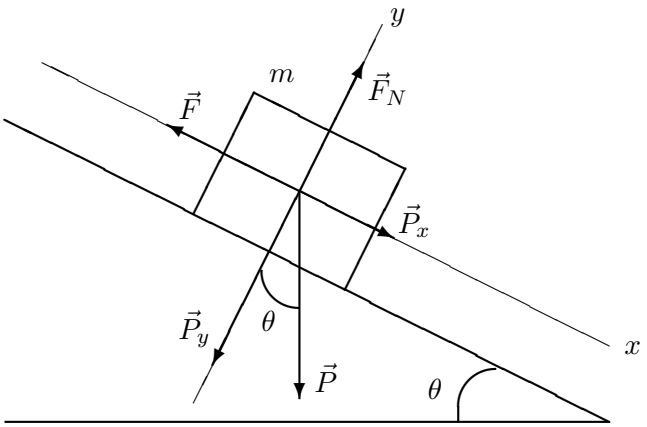

Figure 1: Cube on an inclined plane.

where the x–axis is parallel to the slope of the plane, $P_x = mg\sin(\theta)$ is the projection of the weight $\vec{P}$ on the x–axis, m the mass of the cube, g is gravity, $\ddot{x} = \frac{d^2x}{dt^2}$ (being x the displacement of the cube and t the time), $-F$ the tangential friction force, and θ is the angle that provides the inclination of the plane.

We observe experimentally that for small values of θ the cube does not move. This can be explained by the existence of a force equal to $-\vec{P}_x$: friction. To complete the description of Equation (1), it is necessary to find a description of the force F. The simplest way to describe friction is through the Coulomb model [5, pp. 41–42] (see Figure 2)

$$F = F_c \quad \text{for} \quad \dot{x} > 0, \tag{2}$$

$$F = -F_c \quad \text{for} \quad \dot{x} < 0, \tag{3}$$

$$-F_c \leq F \leq F_c \quad \text{for} \quad \dot{x} = 0, \tag{4}$$

where F_c is the Coulomb friction level.

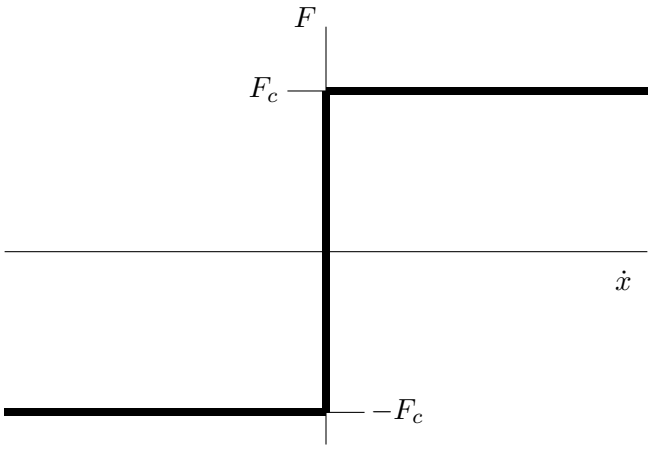

Figure 2: Coulomb model.

The Coulomb model provides a simple way to describe friction, however it fails to reproduce some experimentally observed phenomena. Consider for example the mass m of Figure 3 that

moves to the right towards point A, then moves to the left when it touches point A at some instant time t_A. The Coulomb model predicts that the friction force as a function of time is discontinuous at t_A. This discontinuity of the friction force with respect to time has not been observed experimentally [2, p. 40].

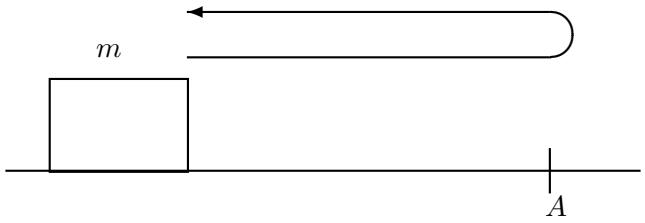

Figure 3: Mass doing the described movement.

One might think to substitute this model with the one of Figure 4 which is continuous with a finite high slope at the origin.

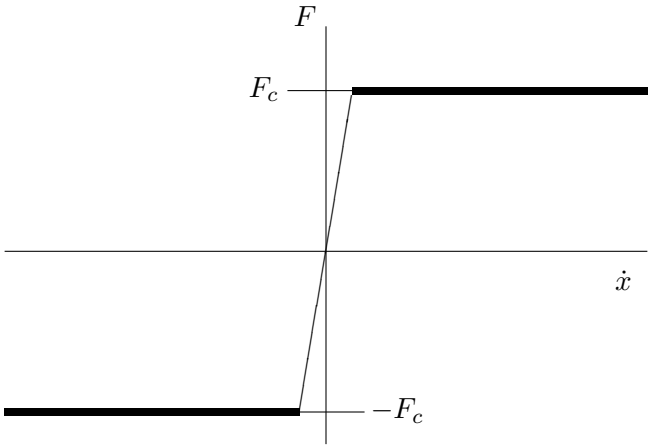

Figure 4: Continuous approximation of the Coulomb model.

However, we show next that this continuous approximation is not compatible with experimental observations.

Indeed, we have said that for small values of θ we observe experimentally that the cube of Figure 1 does not move. This means that $\dot{x} = 0$, which implies that $F = 0$ by using the model of Figure 4. Also, since $\dot{x} = 0$ for all times, it follows that $\ddot{x} = 0$. Substituting in Equation (1) gives $P_x = mg\sin(\theta) = 0$. This is not possible as $m \neq 0$, θ is small but is not zero, and $g \neq 0$. This contradiction means that the continuous approximation of the Coulomb model does not describe the friction behavior.

1.2. The Dahl model

The Dahl model introduced in [6] relates the friction force F to the relative velocity $\dot{x}$ as

$$\frac{dF(x)}{dx} = \sigma \left| 1 - \frac{F}{F_c}\text{sgn}(\dot{x}) \right|^i \text{sgn}\left(1 - \frac{F}{F_c}\text{sgn}(\dot{x}) \right) \tag{5}$$

where $\sigma > 0$ is the rest stiffness, and i a real number. In this paper we consider that $i = 1$ so that the Dahl model becomes

$$\frac{dF(t)}{dt} = \sigma\dot{x}(t) - \sigma\frac{F(t)}{F_c}|\dot{x}(t)|. \tag{6}$$

Defining

$$w(t) = \frac{F(t)}{F_c}, \tag{7}$$

$$\rho = \frac{\sigma}{F_c} > 0, \tag{8}$$

it follows that the Dahl model (6) is described by

$$F(t) = F_c w(t), \tag{9}$$

$$\dot{w}(t) = \rho\big(\dot{x}(t) - |\dot{x}(t)|w(t)\big). \tag{10}$$

In the following, we analyze the compatibility of the Dahl model with the observed behavior in the experiment of Figure 1. Since the displacement x is equal to a constant (the cube does not move), it follows that $\dot{x}(t) = 0, \forall t \geq 0$. Using equation (10) it follows that $w(t) = w(0), \forall t \geq 0$ so that by equation (9) we have $F(t) = F_c w(0), \forall t \geq 0$. Now, the Dahl model is seen as an extension of the Coulomb model so that we expect that equation (4) holds also for the Dahl model. We get $-F_c \leq F(t) = F_c w(0) \leq F_c$ which implies that

$$-1 \leq w(0) \leq 1. \tag{11}$$

Equation (11) is a necessary condition that ensures the compatibility of the Dahl model both with the Coulomb model and with the observed behavior in the experiment of Figure 1.

We need now to check that the Dahl model is also compatible with Equations (2) and (3) which are obtained from the Coulomb model and are confirmed by experiments [5, p. 44–45]. This is done in Section 2.1. It is shown that, if $-1 \leq w(0) \leq 1$, then $|F(t)| \leq F_c, \forall t \geq 0$ and $\lim_{t\to\infty} F(t) = F_c\,\text{sgn}(\dot{x})$ where sgn is the sign function.

Finally, it is shown in [8] that the solution of the differential equation (10) exists and is unique on $\mathbb{R}_+$ so that w is continuous on $\mathbb{R}_+$. This means that the friction force (9) given by the Dahl model is continuous as a function of time, which resolves the above-mentionned inconsistency of the Coulomb model.

1.3. Problem statement

The objective of this paper is to present a new methodology for the identification of the parameters of the Dahl model. Identification consists in designing an experiment or a set of experiments in which the displacement is proposed by the designer, the friction force is measured and an algorithm is proposed by the designer in order to determine the unkown parameters F_c and ρ. The difficulty lies in that w is an internal variable that is not accessible to measurements, and in the fact that the Dahl model is nonlinear.

An extensive survey of the literature dedicated to this specific problem is given in [9] so that we focus here on the main following issues:

(i) Many research works repose heavily on numerical simulations without providing mathematical proofs that the identified parameters are the true ones (see for example [11]).

(ii) In some papers where these proofs have been carried out, the identification technique uses the derivative of measured signals (see for example [7]), which is a method sensitive to noise.

The objective of this paper is to propose a new identification method for the Dahl model that does not use any derivative of measured signals, and with a rigorous proof that the identified parameters are the true ones in the absence of noise.

2. Identification method

Before presenting the identification method, we remind the following facts. In Equations (9)–(10),

(i) the displacement input x is assumed to be accessible to measurements and it can be imposed by the designer,

(ii) the output force F is assumed to be accessible to measurements,

(iii) and the state w may not be accessible to measurements.

The identification method is done in two stages. In the first stage, the parameter F_c is determined using the classical technique of fixing the velocity to some value and measuring the obtained force. A proof is provided to back up this technique in the case of the Dahl model. The second stage is based on a the characterization of the hysteresis loop for the Dahl model given in [8].

2.1. First stage: Identification of parameter F_c.

Consider that $\dot{x} = v =$ constant and $v > 0$ (the same analysis applies for $v < 0$). From equation (10) we get:

$$\dot{w}(t) = \rho\big(1 - w(t)\big)\dot{x}(t) \tag{12}$$

Integrating both part of (12) it follows that

$$\int \frac{dw}{1-w} = \int \rho dx \tag{13}$$

which gives

$$-\ln\big(|1-w|\big) = \rho x + C_1 \tag{14}$$

that is,

$$1 - w = \pm e^{-\rho x - C_1} = C_2 e^{-\rho x} \tag{15}$$

where $C_2 = \pm e^{-C_1}$

Finally, we obtain that:

$$w = 1 - C_2 e^{-\rho x}. \tag{16}$$

The constant C_2 can be obtained from (16) as

$$C_2 = (1 - w(0))\, e^{\rho x(0)}. \tag{17}$$

Substituting in Equation (16) gives

$$w(t) = 1 - \big(1 - w(0)\big)e^{-\rho[x(t) - x(0)]}. \tag{18}$$

Since $\dot{x} = v =$ constant, it follows that $x(t) = vt + x(0)$ so that

$$w(t) = 1 - \big(1 - w(0)\big)e^{-\rho v t}. \tag{19}$$

Since $\rho > 0$ and $v > 0$, it follows from equation (19) that $\lim_{t\to\infty} w(t) = 1$. Combining this fact with Equation (9), it follows that F_c can be estimated through

$$F_c = \lim_{t\to\infty} F(t). \tag{20}$$

Finally observe that, if $-1 \le w(0) \le 1$, then $0 \le 1 - w(0) \le 2$ so that $-1 \le 1 - (1 - w(0))e^{-\rho v t} \le 1$. This means that $|F(t)| \le F_c, \forall t \ge 0$.

2.2. Second stage: Identification of parameter ρ

Note that, once F_c identified, w can be determined using Equation (9) as $w = \frac{F}{F_c}$. One may think that ρ can be obtained from Equation (10) as $\rho = \frac{\dot{w}(t)}{\dot{x}(t) - |\dot{x}(t)|w(t)}$. However, this would mean that we are using the derivative of w, that is the derivative of F. The aim of the present paper is precisely to avoid the use of the derivative of functions obtained from experiments because these derivatives are usually corrupted by noise.

Definition 1 *[8] Let $T > 0$. A T-periodic function $x\colon \mathbb{R}_+ \to \mathbb{R}$ is said to be wave periodic if there exists some $T^+ \in (0, T)$ such that:*

- *The function x is continuous on $\mathbb{R}_+$.*
- *The function x is continuously differentiable on $(0, T^+)$ and on (T^+, T).*
- *The function x is strictly increasing on $(0, T^+)$ and is strictly decreasing on (T^+, T).* ■

To describe the hysteresis loop of the Dahl model (9)–(10), define the following functions:

$$\begin{aligned} \varphi_{1,1}^+ &: (-1, 1) \to \mathbb{R} \\ \varphi_{1,1}^+(\alpha) &= \int_0^\alpha \frac{du}{1-u} = -\ln(1-\alpha). \end{aligned} \tag{21}$$

$$\begin{aligned} \psi_{1,1}^+, \psi_{1,1} &: \mathbb{R} \to \mathbb{R} \\ \psi_{1,1}^+(\beta) &= \frac{e^\beta - 1}{e^\beta}, \end{aligned} \tag{22}$$

$$\psi_{1,1}(\beta) = \frac{e^\beta - 1}{e^\beta + 1}. \tag{23}$$

Theorem 1 *[8] Consider the Dahl model (9)–(10). Let x be a wave periodic displacement input as in Definition 1. Define the functions $w_m : [0, T] \to \mathbb{R}$ for any non-negative integer m as follows*

$$w_m(\tau) = w(mT + \tau), \quad \tau \in [0, T]. \tag{24}$$

Then,

(a) The sequence of functions $\{w_m\}_{m\ge 0}$ converges uniformly on the interval $[0, T]$ to a continuous function $\bar{w} : [0, T] \to \mathbb{R}$ defined by

$$\bar{w}(\tau) = \psi_{1,1}^+\big[\gamma + \rho\big(x(\tau) - X_{\min}\big)\big], \forall \tau \in [0, T^+], \tag{25}$$

$$\bar{w}(\tau) = -\psi_{1,1}^+\big[\gamma - \rho\big(x(\tau) - X_{\max}\big)\big], \forall \tau \in [T^+, T], \tag{26}$$

$$\gamma = \varphi_{1,1}^+\big[-\psi_{1,1}\big(\rho\,(X_{\max} - X_{\min})\big)\big]. \tag{27}$$

(b) For all $\tau \in [0, T]$, we have

$$-1 < -\psi_{1,1}(\rho(X_{\max} - X_{\min})) \leq \bar{w}(\tau), \tag{28}$$

$$\bar{w}(\tau) \leq \psi_{1,1}(\rho(X_{\max} - X_{\min})) < 1, \tag{29}$$

the lower and the upper bounds of $\bar{w}(\tau)$ being attained at $\tau = 0$ and $\tau = T^+$ respectively. ■

The objective of this section is to use Theorem 1 as a basis for an identification method of the unknown parameter ρ. To this end, define

$$a = \frac{2}{1 + e^{-\rho(X_{\max} - X_{\min})}}. \tag{30}$$

Then, from Equation (27) it follows that

$$\begin{aligned} \gamma &= -\ln\left(1 + \psi_{1,1}\left[\rho\left(X_{\max} - X_{\min}\right)\right]\right) \\ &= -\ln\left(1 + \frac{e^{\rho(X_{\max} - X_{\min})} - 1}{e^{\rho(X_{\max} - X_{\min})} + 1}\right) \\ &= -\ln(a) \end{aligned} \tag{31}$$

where Equations (21), (23) and (30) have been used. From Equation (31) we obtain

$$\begin{aligned} \psi_{1,1}^{+}\left[\gamma + \rho\big(x(\tau) - X_{\min}\big)\right] &= \psi_{1,1}^{+}\left[-\ln(a) + \rho\big(x(\tau) - X_{\min}\big)\right] \\ &= 1 - e^{\ln(a) - \rho(x(\tau) - X_{\min})} \\ &= 1 - ae^{-\rho(x(\tau) - X_{\min})}. \end{aligned} \tag{32}$$

Observe that the steady–state force $\bar{F}$ is given by $\bar{F}(\tau) = F_c\,\bar{w}(\tau), \forall \tau \in [0, T]$. Thus, it follows from Equation (32) that Equation (25) can be written as

$$\bar{F}(\tau) = F_c\left(1 - ae^{-\rho(x(\tau) - X_{\min})}\right), \quad \forall \tau \in [0, T^+]. \tag{33}$$

In a similar vein, Equation (26) can be written as

$$\bar{F}(\tau) = F_c\left(-1 + ae^{\rho(x(\tau) - X_{\max})}\right), \quad \forall \tau \in [T^+, T]. \tag{34}$$

Observe that the displacement function x is bijective on the time interval $[0, T^+]$ since it is continuous and strictly increasing. This means that to each value of τ corresponds a unique value $x(\tau)$, which provides a unique value of $\bar{F}(\tau)$ through Equation (33). This in turn means that to each displacement value $x \in [X_{\min}, X_{\max}]$ corresponds a unique value of the friction force in steady–state given by $F_c\left(1 - ae^{-\rho(x - X_{\min})}\right)$. We denote this last quantity $\bar{F}_{\uparrow}(x)$ where the index $\uparrow$ sets for loading (that is an increasing displacement). Thus Equation (33) can be written as

$$\bar{F}_{\uparrow}(x) = F_c\left(1 - ae^{-\rho(x - X_{\min})}\right), \quad \forall x \in [X_{\min}, X_{\max}]. \tag{35}$$

Observe that, by an abuse of notation, the displacement x in Equation (33) is a function from $[0, T^+]$ to $\mathbb{R}$ whilst the same notation is used in Equation (35) to denote some real number in the interval $[X_{\min}, X_{\max}]$. In a similar vein, Equation (34) can be written as

$$\bar{F}_{\downarrow}(x) = F_c\left(-1 + ae^{\rho(x - X_{\max})}\right), \quad \forall x \in [X_{\min}, X_{\max}] \tag{36}$$

where the index $\downarrow$ sets for unloading (that is a decreasing displacement). In both equations (35) and (36), the bar over the symbol F means that the force is the one obtained in "steady–state". Equations (35)–(36) describe the hysteresis loop of the Dahl model and are the basis for the identification methodology of the parameter ρ.

Consider the point $x_1 = \frac{X_{\max}+X_{\min}}{2} + \alpha$ and compute $\bar{F}_\uparrow$ at that point using Equation (35). We obtain:

$$\bar{F}_\uparrow(x_1) = F_c \left(1 - ae^{-\rho(X_{\max}-X_{\min}+2\alpha)}\right). \tag{37}$$

Now, consider the point $x_2 = \frac{X_{\max}+X_{\min}}{2} - \alpha$ and compute $\bar{F}_\downarrow$ at that point using Equation (36). We obtain:

$$\bar{F}_\downarrow(x_2) = F_c \left(-1 + ae^{-\rho(X_{\max}-X_{\min}+2\alpha)}\right). \tag{38}$$

It can be seen that $\bar{F}_\uparrow(x_1) = -\bar{F}_\downarrow(x_2)$ which means that the hysteresis loop of the Dahl model is symmetric with respect to the point $\left(\frac{X_{\max}+X_{\min}}{2}, 0\right)$ (see Figure 5).

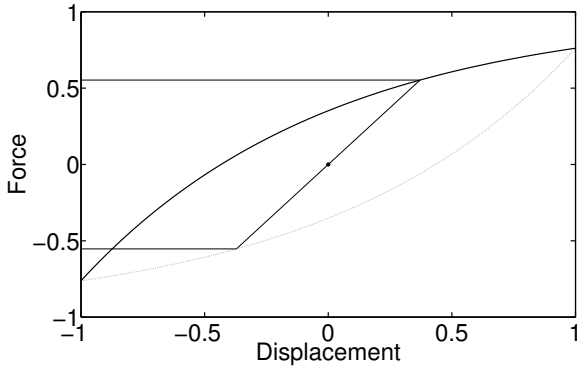

Figure 5: Solid line: $\bar{F}_\uparrow(x)$ versus displacement x.
Dotted line: $\bar{F}_\downarrow(x)$ versus displacement x.
The marker corresponds to the point $\left(\frac{X_{\max}+X_{\min}}{2}, 0\right)$.

This symmetry property is used to estimate parameter ρ using only function $\bar{F}_\uparrow(x)$. By Equation (35) we obtain:

For $x = X_{\min}$

$$\rho = \frac{\ln\left(\frac{1+\frac{\bar{F}_\uparrow(X_{\min})}{F_c}}{1-\frac{\bar{F}_\uparrow(X_{\min})}{F_c}}\right)}{X_{\min} - X_{\max}}. \tag{39}$$

For $x = X_{\max}$

$$\rho = \frac{\ln\left(\frac{1-\frac{\bar{F}_\uparrow(X_{\max})}{F_c}}{1+\frac{\bar{F}_\uparrow(X_{\max})}{F_c}}\right)}{X_{\min} - X_{\max}}. \tag{40}$$

Finally, for $x = \frac{X_{\max}+X_{\min}}{2}$

$$\rho = \frac{2\ln\left(\dfrac{1-\sqrt{1-\left(1-\dfrac{\bar{F}_{\uparrow}\left(\frac{X_{\max}+X_{\min}}{2}\right)}{F_c}\right)^2}}{1-\dfrac{\bar{F}_{\uparrow}\left(\frac{X_{\max}+X_{\min}}{2}\right)}{F_c}}\right)}{X_{\min}-X_{\max}}. \tag{41}$$

3. Numerical simulations

The aim of this section is to illustrate the identification methodology of Section 2 by means of numerical simulations. To this end, we consider a Dahl model (9)–(10) with the following values of its parameters: $F_c = 1$ and $\rho = 1$. As explained in Section 2, our identification method proceeds in two stages:

(i) In the first stage the parameter F_c is identified using Equation (20).

(ii) In the second stage, that value of F_c is used to determine parameter ρ using any of Equations (39), (40) or (41).

3.1. First stage: Identification of parameter F_c.

In this stage we choose a displacement function $x(t) = t$ (see Figure 6) which means that the corresponding velocity $\dot{x}$ is constant and equals 1. The state $w(t)$ is computed by solving the

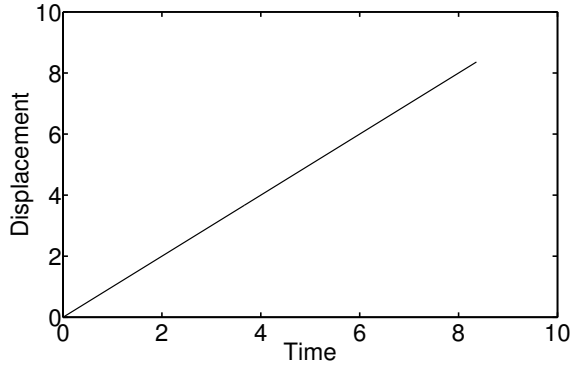

Figure 6: Displacement $x(t)$ versus time $t \in \mathbb{R}_+$.

differential equation (10) using Matlab solver ode23s with an initial condition $w(0) = 0$. The corresponding force $F(t)$ is then calculated using Equation (9) and is plotted in Figure 7. The parameter F_c is calculated using Equation (20), and we obtain $F_c = 1$.

3.2. Second stage: Identification of parameter ρ

In this stage we choose a displacement function $x(t) = -\cos(t)$ (see Figure 8). Observe that x is a wave periodic function (see Definition 1) with $T = 2\pi$ and $T^+ = \pi$. Again, the state $w(t)$ is computed by solving the differential equation (10) using Matlab solver ode23s with an initial condition $w(0) = 0$. The corresponding force $F(t)$ is then calculated using Equation (9) and is plotted in Figure 9.

The identification methodology uses the *steady–state* response of the force to determine the unknown parameter ρ. We consider that the steady–state is attained at the fourth period (see Figure 9), and is plotted in Figure 10 as steady–state force $\bar{F}(\tau)$ versus time τ.

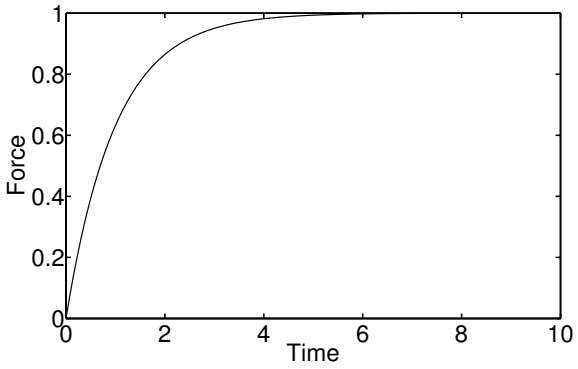

Figure 7: Force $F(t)$ versus time $t \in \mathbb{R}_+$.

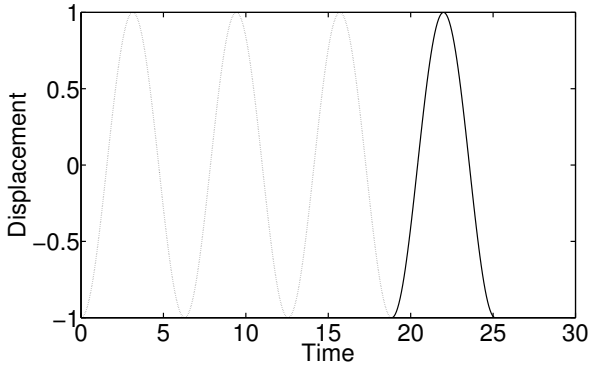

Figure 8: Displacement $x(t)$ versus time $t \in \mathbb{R}_+$.

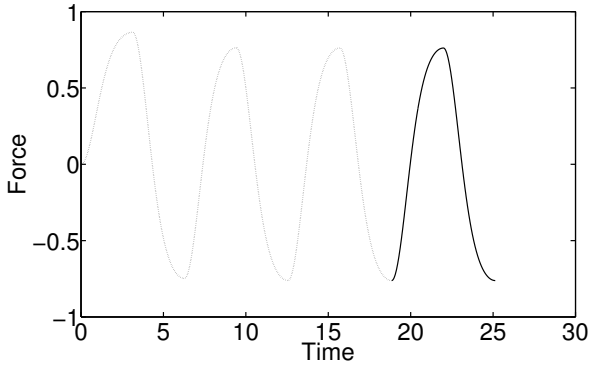

Figure 9: Force $F(t)$ versus time $t \in \mathbb{R}_+$.
Dotted line: Transient response.
Solid line: Steady–state response.

It is again plotted in Figure 11 where, in this case, the solid line corresponds to the increasing part of the force which is the part that is used to find the parameter ρ.

Now that the plot $\bar{F}_\uparrow(x)$ versus x is available, we obtain the value $\bar{F}_\uparrow(X_{\min})$ which provides the parameter ρ through Equation (39). Similarly, the value $\bar{F}_\uparrow(X_{\max})$ provides the parameter ρ through Equation (40), whilst the value $\bar{F}_\uparrow\left(\frac{X_{\max}+X_{\min}}{2}\right)$ provides the parameter ρ through

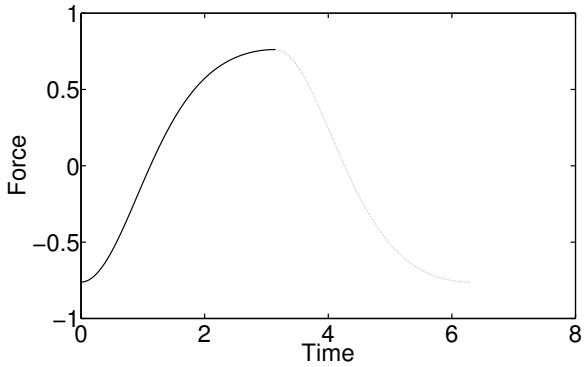

Figure 10: Steady–state force $\bar{F}(\tau)$ versus time $\tau \in [0, T]$.
Solid line: Loading.
Dotted line: Unloading.

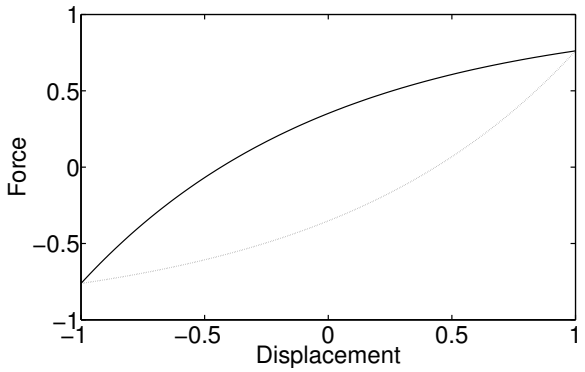

Figure 11: Steady-state force $\bar{F}(\tau)$ versus displacement $x(\tau)$, $\tau \in [0, T]$.
Solid line: $\bar{F}_{\uparrow}(x)$ versus displacement x.
Dotted line: $\bar{F}_{\downarrow}(x)$ versus displacement x.

Equation (41). In the three cases we find $\rho = 1$.

4. Conclusion

This paper presents a new method for the parametric identification of the Dahl model. The method consists of two stages: in each stage a special kind of displacement is imposed, and the steady–state force that corresponds to that displacement is collected. As a future research line, the authors aim to carry out experiments to apply the method to the modeling of large-scale magnetorheological dampers using a viscous plus Dahl model.

4.1. Acknowledgments

Supported by the Spanish Ministry of Economy and Competitiveness of through grant DPI2011-25822 and by the Spanish Ministry of Education, Culture and Sport through a "scholarship of collaboration in university departments". The scholarship is approved by the Universitat Politècnica de Catalunya and managed by the AGAUR (Agency for Management of University and Research Grants). We also acknowledge the support of the AGAUR through the grant 2014 SGR 859 to the research group CoDAlab.

References

[1] Aguirre N, Ikhouane F, Rodellar J and Christenson R 2012 Parametric identification of the Dahl model for large scale MR dampers *Struct. Control Health Monit.* **19** pp 332–347

[2] Armstrong-Helouvry B 1991 *Control of Machines with Friction* Kluwer Academic Publishers.

[3] Armstrong-Helouvry B, Dupont P and Canudas De Wit C 1994 A survey of models, analysis tools and compensation methods for the control of machines with friction *Automatica* **30(7)** pp 1083–1138

[4] Carvalho-Bittencourt A and Gunnarsson S 2012 Static friction in a robot joint-modeling and identification of load and temperature effects *J. Dyn. Sys., Meas., Control* **134(5)** pp 051013-1–051013-10

[5] Coulomb C A 1821 *Théorie des Machines Simples, en Ayant Égard au Frottement de Leurs Parties et à la Roideur des Cordages* [in Gallica, Bibliothèque Nationale de France] Paris France

[6] Dahl P 1976 Solid friction damping of mechanical vibration *AIAA J.* **14** pp 1675–1682

[7] Ikhouane F. and Gomis-Bellmunt O 2008 A limit cycle approach for the parametric identification of hysteretic systems *Systems & Control Letters* **57** pp 663–669

[8] Ikhouane F and Rodellar J 2005 On the hysteretic Bouc-Wen model. Part I: forced limit cycle characterization *Nonlinear Dyn.* **42** pp 63–78

[9] Ismail M, Ikhouane F and Rodellar J 2009 The hysteresis Bouc-Wen model, a survey *Arch Comput Methods Eng 16* pp 161–188

[10] Jrad H, Renaud F, Dion J L, Tawfiq I and Haddar M 2013 Experimental characterization, modeling and parametric identification of the hysteretic friction behavior of viscoelastic joints *Int. J. Appl. Mech.* **5(2)** 1350018 (21 pages)

[11] Piatkowski T 2014 Dahl and LuGre dynamic friction models – The analysis of selected properties *Mechanism and Machine Theory* **73** pp 91–100